

I. A. Petrusha, D. Sc.<sup>1</sup>; B. S. Sadovyi, Ph.D.<sup>2,3</sup>, P. S. Sadovyi, Eng.<sup>2</sup>;  
A. S. Osipov, Yu. Yu. Rumiantseva, Ph. D.<sup>1</sup>; P. A. Balabanov, Ph. D.<sup>4</sup>; P. Klimczyk, D. Sc.<sup>5</sup>;  
Yu. I. Sadova, Ph. D. Student<sup>1</sup>, O. V. Savitskyi, S. O. Hordieiev, T. O. Sakal, Junior Researchers<sup>1</sup>

<sup>1</sup>V.M. Bakul Institute for superhard materials of the National Academy of Sciences of Ukraine, 2, Avtozavodska str., 04074 Kyiv, Ukraine, e-mail: dialab@ism.kiev.ua

<sup>2</sup>Institute of High Pressure Physics, Polish Academy of Sciences, 29/37, Sokolowska str., 01-142 Warsaw, Poland, e-mail: bsad@unipress.waw.pl

<sup>3</sup>Faculty of Ivan Franko National University of Lviv, 8, Kyryla i Mefodiya str., Lviv, 79005, Ukraine, e-mail: bogdan.sadovyi@lnu.edu.ua

<sup>4</sup>EcoDiamond GmbH, Silder Moor 3, 18196, Dummerstorf, Germany, e-mail: pavlo@ecodiamond.eu

<sup>5</sup>Institute of Advanced Manufacturing Technology, Wroclawska 37A, 30-011 Kraków, Poland, e-mail: piotr.klimczyk@kit.lukasiewicz.gov.pl

## INVESTIGATION OF GaN BEHAVIOR IN CONTACT WITH FE, Fe<sub>2-4</sub>N AND Co/Cr AT HIGH PRESSURES AND HIGH TEMPERATURES

*In this work behavioral features of gallium nitride (GaN) being in contact with Fe, Fe<sub>2-4</sub>N and (Co/Cr)<sub>eut</sub> under high-pressure (6–8 GPa) high-temperature (up to 2000 °C) conditions (HP-HT) have been described. Preparatory stages of experimental research including thermobaric calibration of the toroidal HP apparatus using thermocouple method considering some melting results of a number of metals and alloys such as Pt, (Mo–C)<sub>eut</sub>, Fe, Fe<sub>2-4</sub>N, (Co/Cr)<sub>eut</sub>, Cu and Pr under pressure are highlighted in detail. The gallium nitride was found to dissolve in the Fe, Fe<sub>2-4</sub>N and (Co/Cr)<sub>eut</sub> melts as evidenced by increasing of sample weights (non GaN part). As a rule, changes of mass took place starting from temperatures below the melting point of a pure material (sample) that is obviously due to contact melting at the GaN-sample interface. At a fixed pressure and isochronous experimental conditions the degree of GaN dissolution strongly depends from temperature for all systems under consideration. For temperature region of 1800–2000 °C a mass increasing of the second component in GaN–Fe, GaN–Fe<sub>2-4</sub>N and GaN–(Co/Cr)<sub>eut</sub> pairs due to GaN dissolving reach 20–30 wt. %. There was a tendency to decreasing of GaN solubility coursed by pressure reducing as it was noted on example of the GaN–(Co/Cr)<sub>eut</sub> pair. Regarding the equilibrium concentrations of Ga and N in melts of Fe, Fe<sub>2-4</sub>N and (Co/Cr)<sub>eut</sub> alloy the final conclusion will be received after examination of quenched samples by EDX, XRD, Raman spectroscopy and other methods.*

**Key words:** gallium nitride, high pressure and high temperature, contact melting, dissolution in melts, iron, iron nitride, (Co/Cr)<sub>eut</sub> alloy

Studies of the physicochemical processes of the interaction of gallium nitride (GaN) with melts of metals and alloys (*Me*) at high pressures and temperatures are important in the context of highly efficient growth systems search both spontaneous mass crystallization and the perfect GaN crystals growing by temperature gradient methods. It is advisable to study the behavior of GaN–*Me* systems at temperatures exceeding the contact melting ones using toroidal apparatus with special designs of high-pressure cells (HPC). This work describes in detail the preparatory stages of the experimental research including the calibration of the high-pressure apparatus (*HPA*) for temperature and pressure. A relatively simple methodology was used to study the thermobaric behaviors of a number of *Me* and GaN–Fe, GaN–Fe<sub>2-4</sub>N and GaN–(Co/Cr)<sub>eut</sub> contact pairs. The composition of the cobalt-chromium alloy corresponded to the eutectic containing 46.5 at. % Cr. The degree of GaN dissolution was evaluated on the basis of the change in the weight of the *Me* samples *post factum*.

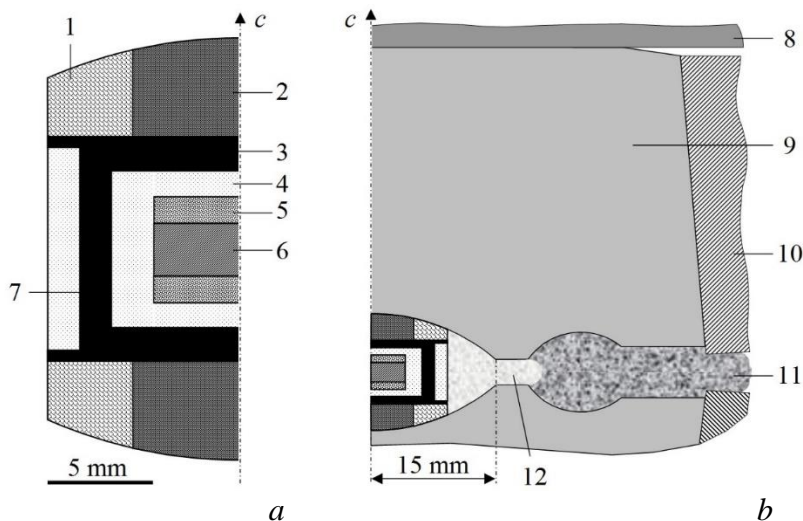


Fig. 1. Central part (half axial section) of HPC assembly (a) and formation of a locking system (deformable seal) at compression of HPAT-30 (b): a – location of parts in HPC (1 – heat insulating pyrophyllite ring; 2 – axial heater pressed from natural low-ash graphite mixed with 40 vol. % ZrO<sub>2</sub>; 3 – pressed caps of natural low ash graphite; 4 – pressed capsule of CsCl mixed with 10 wt. % ZrO<sub>2</sub>; 5 – GaN powder; 6 – sample of Fe, Fe<sub>2</sub>-4N or (Co-Cr)eut alloy; 7 – cylindrical heater made of electrode graphite grade R8710 (SIGRAFINE, bulk density  $d = 1.88 \text{ g/cm}^3$ ); b – deformable seal formation at c-axis compression of the apparatus (8 – bearing plate, 9 – hard alloy inserts, 10 – fastening steel ring, 11 – external deformable seal (pressed calcite), 12 – zone of internal deformable seal (bulk lithographic stone)

Having been used technique gives way to make samples convenient for subsequent electron microscopic studies.

The necessary HP–HT conditions were created using a toroidal type apparatus of the «HPAT-30» model [1]. The available level of  $p, T$ -parameters for HPAT-30 is usually limited by a pressure of about 8 GPa and a temperature of 2400 °C. The volume of the high-pressure zone is determined by the dimensions of the spherical cavity volume (segments) in the oppositely directed carbide inserts of the apparatus. The segment base diameter is 30 mm and a sphere radius is 22,5 mm. In the initial state, after the placement of the HPC, the distance between the bases of the segments is 8.3 mm. In the compressed apparatus, after the convergence of the inserts, it is approximately 2,7 mm (fig. 1).

HPAT-30 assumes the use of the DO-043 model press

to reach necessary nominal axial loading force  $F = 16.35 \text{ MN}$  at oil pressure in the plunger system equal to 101,3 MPa. When high pressure is created, deformable interlayers in the zones of the inner and outer seals prevent possible depressurization of the device, and also block the radial outflow of materials from the central zone of the HPC, where the sample in the capsule and the graphite heater are located (see fig. 1).

*Specificities of HPAT-30 temperature calibration with evaluating of the pressure at a high-temperature range.* Two methods of temperature calibration were used. In the first, the standard approaches with applying of thermocouple sensor were used [2]. In the second, melting of the substances depending on pressure was took into consideration. The coordination of results obtained makes it possible to estimate the magnitude of pressure at high temperatures.

At thermocouple calibration the junction of Pt–Rh (30 wt. %) and Pt–Rh (6 wt. %) electrodes was located in the center of the HPC which was filled by graphite-like boron nitride in the form of a compacted powder to a density of  $d \cong 1,8 \text{ g/cm}^3$ . The electrodes were placed in a ceramic case made of Al<sub>2</sub>O<sub>3</sub> in order to exclude the shunting of the measuring circuit by the heater. The determination of the temperature depending on the power of the electric current of the heater was carried out in 6 independent similar experiments. Compilation of the obtained data was used to construct a calibration curve by means of polynomial approximation (fig. 2).

The analytical expression for the obtained approximate relation has the form of a polynomial

$$T(P) = 17,18456 + 0,2414 \cdot P + 1,48784 \cdot 10^{-5} \cdot P^2, \quad (1)$$

where  $T$  – temperature, °C;  $P$  – electrical power, W.

For temperatures exceeding 1900 °C an extrapolation was used, according to an approximation (1). As seen in fig. 2, in the temperature range 1200–2400 °C linear approximation

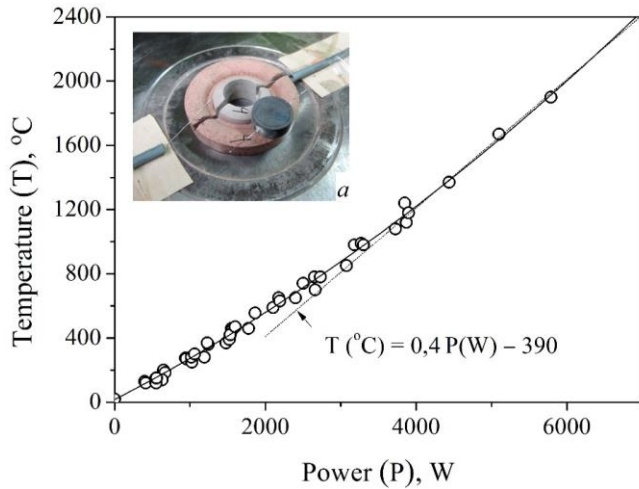


Fig. 2. Temperature calibration graph of HPAT-30 for the HPC center, depending on the current power in the heater: a – introduction of a thermocouple followed by diametrical wiring of thermoelectrodes

$T(P) = 0,4 \cdot P - 390$  is entirely applicable. Therefore a change in power of 100 W causes a temperature change about 40 °C. Note that automated power control system used in this research has allowed to set and maintain electrical power in increments of 1 W, which at above temperature range corresponds to  $\Delta T(P) \cong 0,4$  °C.

The real pressure in the cell at high temperatures was estimated based on the known data on Pt melting [3] and contact eutectic melting in the Mo–C system [4–6]. The procedure consisted in the experimental determination of the temperature interval  $\Delta T$  between the melting points of Pt and  $(\text{Mo-C})_{\text{eut}}$ , knowing which it is possible to determine the pressure in the HPC (fig. 3).

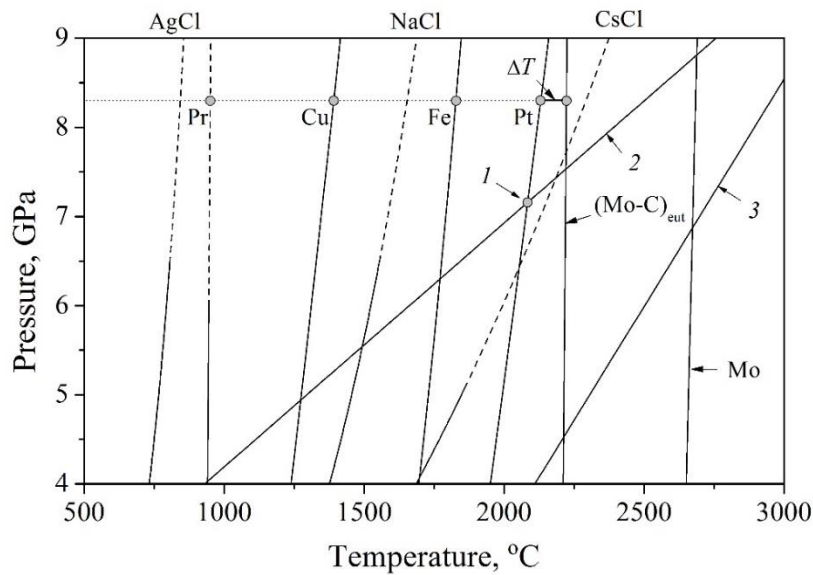


Fig. 3. Melting lines of substances: 1 – intersection of the Pt melting line with the diamond-graphite equilibrium line (2) [7], which defines the reference point with coordinates  $T = 2084$  °C and  $p = 7.15$  GPa; 3 – line of decomposition of GaN [8]; data for metals Pr, Cu and Fe, as well as chlorides Ag, Na and Cs, are borrowed from reviews of E. Yu. Tonkov [9]. The interval  $\Delta T = 90$  °C corresponds to the pressure in the cell  $p \cong 8.3$  GPa

About parameters of thermobaric action were also judged based on analysis of data on Me melting taking into account the known  $T_m(p)$  dependences – Fe, Al, and Pr [9]; Ni and Cu [3] (fig. 3). Note that the melting points of praseodymium and eutectic  $(\text{Mo-C})_{\text{eut}}$  are practically independent of pressure.

Sodium chloride or the CsCl–NaCl salt system which forms a low-melting eutectic with 35,5 mol. % NaCl was used as a flux. At normal pressure the melting point of the eutectic is 495 °C [10]. In the case of fusible Pr a silver chloride is the most suitable medium having a lower melting point. The  $T_m(p)$  dependence for CsCl is known up to 5 GPa, for Pr up to 6 GPa, and for AgCl and NaCl up to 6,5 GPa [9]. Data shown in fig. 3 for these substances (dotted lines) are calculated in the first approximation using adequate extrapolation of the approximating functions obtained by mathematical processing of the available experimental data.

The *Me* samples, usually in the form of small fragments (pieces) of irregular shape ranging in size from 1 to 3 mm, were pressed into the salt using a steel mold making close to non-porous «sample melting module». The module was inserted into the capsule (4) instead of GaN (5) and sample (6) (see fig. 1, a). In some cases, a small amount of 0,3–0,4 mm diamond crystals were placed in the salt together with the Fe, Pt, and Mo samples. For experiments with Mo eutectic melting the cylindrical samples of 3,7 mm in diameter and of 3 mm in thickness were prepared. The Pt samples had equal diameter and thickness about 2 mm. The cylinders by a flat surface were mounted on a 0,5 mm thick substrate from low-ash crystalline graphite placed at the bottom of the capsule.

In all experiments the compression force of the HPA was kept constant at the nominal value  $F = 16.35$  MN. The duration of the thermobaric action was 90 s. Determination of the electric power value at which the sample begins to melt involves performing several experiments with successive narrowing of the uncertainty interval  $\Delta P$  (bisection method). After completion of the experiment, the sample was removed from the salt by dissolving it in water. Post factum the melting of metals was indicated by a change in the shape of the samples – the appearance of convex areas on flat surfaces, rounding of sharp tops and edges, folding into a drop, and smoothing of the roughness profiles during contact melting. Under thermobaric action the hydrostatic compression conditions are realized in molten salts. In liquid media the effects of convective and gravitational migration of samples in the flux melt are also possible. Usually under the action of gravitational forces *Me* samples, which have a higher density in comparison with the density of the salt melt, sank to the bottom of the capsule.

Many characteristic features of the behavior of above metals make it possible to draw quite definite conclusions regarding the conditions of thermobaric action, as can be seen below in the text. The methodological approach proposed in the work assumes the uniformity of the HPC design, the invariability of the geometric parameters of the parts in the assemblies and the materials used, in particular the maximum possible similarity of heaters made of high-quality electrode graphite of the R8710 type (SIGRAFINE, bulk density  $d = 1,88$  g/cm<sup>3</sup>). Of course, all these factors, along with the technical state of the HPAT-30, can have a significant effect on the convergence of the experimental results.

Contact eutectic melting in Mo–C and Pt–C systems. At temperatures not high enough to melt pure Mo the effect of eutectic melting in contact with the graphite – C(gr), substrate can be so significant that the resulting melt begins to behave like a diamond-producing catalyst-solvent. The infiltration process of melt penetration under the action of high pressure covered a significant part of the substrate volume. As a result, a spontaneous mass crystallization of diamond was observed with the formation of a strong intergrowth in the form of a fine-grained «diamond brush» concentrically located around the edge of the sample. In this case, the upper part of the Mo sample retained its cylindrical shape without any signs of metal melting (fig. 4, a). In the next series of experiments, narrowing the range of uncertainty in the electrical power of the heater  $\Delta P$  in accordance with bisection method scheme, the value of  $P$  was recorded, at which the first signs of contact melting appeared – smoothing of the roughness profile on the sample surface in the absence of diamond formation (fig. 4, b, c).

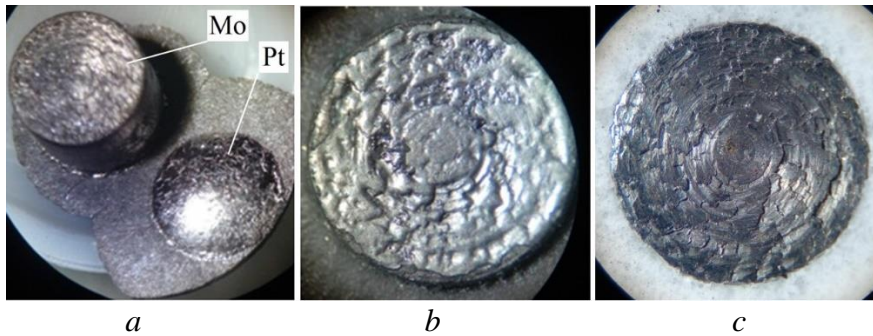


Fig. 4. Contact melting in the Mo-C(gr) and Pt-C(gr) systems: a – infiltration of diamond-producing melts into the graphite substrate, facilitating the process of catalytic conversion of graphite into diamond by forming a fine-grained «diamond brush» under the samples; b – smoothing of the Mo surface roughness profile at the moment of the start of contact melting at a lower temperature; c – roughly processed surface of the initial Mo sample

Melting of platinum in contact with graphite proceeds at significantly lower temperatures in comparison with (Mo-C)<sub>eut</sub>. Note that at normal pressure the melting plateau in the Pt-C system corresponds to the eutectic point at a temperature of 1737,4 °C and a carbon content of 1,2 wt. % [11]. The melting point of pure platinum, at least up to a pressure of 9 GPa, is also below than  $T_m(p)$  for (Mo-C)<sub>eut</sub> (see fig. 3). Thus, in conditions of rising temperature, the eutectic melting of Pt precedes the appearance of the melt at the Mo-C(gr) interface. As in the case of Mo, the platinum-carbon melt exhibits significant diamond-producing activity, as a result of which a diamond-containing intergrowth is formed under the molten platinum in the radially expanded area and throughout the entire depth of the graphite substrate (fig. 4, a). Obviously, in these experiments, the parameters of thermobaric action correspond to the region of thermodynamic stability of diamond.

*Melting platinum in the absence of contact with graphite.* After melting in a liquid NaCl medium the Pt melt curls up into a drop which sinks to the bottom of the capsule. In the case of presence of small diamond crystals (0,3–0,4 mm) initially placed under the capsule lid, they sink in salt and after colliding with a Pt drop are held on its surface due to the action of adhesion forces (flotation effect). It can be seen that the crystals are predominantly concentrated on top of the drop, i. e. «float» on the surface of the molten metal due to the lower density of diamond in relation to the density of platinum in the liquid state (fig. 5).

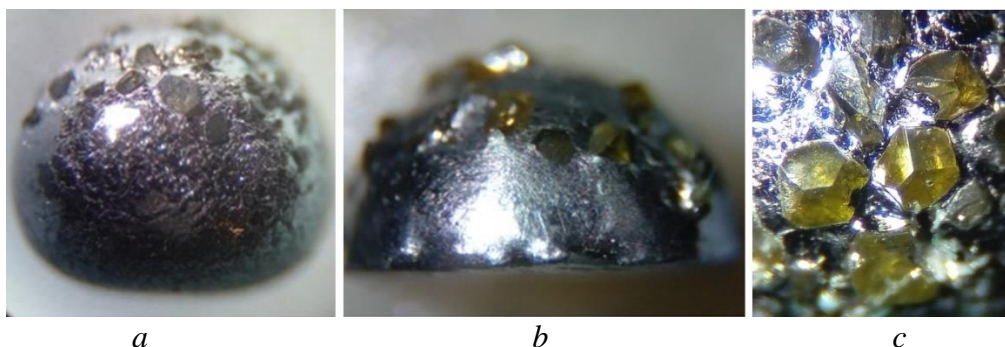


Fig. 5. Drops of platinum with diamond single crystals (samples solidified at the bottom of the capsule in an NaCl medium upon cooling the HPC). A current power in the heater: a –  $P = 6.8$  kW; b, c –  $P = 6.5$  kW; c – absence of any signs of diamond graphitization

Graphitization of diamond in contact with a platinum melt-solvent of carbon is not observed. Therefore it can be argued that the system in terms of  $p, T$ -parameters is above the control point (1) in

the upper right sector between the line  $T_m(p)$  of platinum and the line of diamond-graphite equilibrium [7] (see fig. 3).

Processing of the experimental results on fixing the moments of the onset of melting of Pt and  $(\text{Mo-C})_{eut}$ , taking into account the data of thermocouple HPC calibration (see fig. 2), showed that the difference between the corresponding temperatures is  $\Delta T_m(p) \cong 90 \pm 10$  °C (see fig. 3), which in turn determines the pressure in the cell  $p \cong 8,3 \pm 0,3$  GPa at high temperatures in accordance with the analytical relation

$$\Delta T_m(p) = 2473,15 - 2042(p/21,5 + 1)^{1/2} + 2,7p, \quad (2)$$

which is based upon data from [3, 5] and where  $T$  – temperature, °C;  $p$  – pressure, GPa.

An intense spontaneous nucleation and grows of diamonds in the Fe–C(gr) system developed in the contact zone of the iron sample with graphite and it also indicates a high level of pressure in the cell at high temperatures (fig. 6).

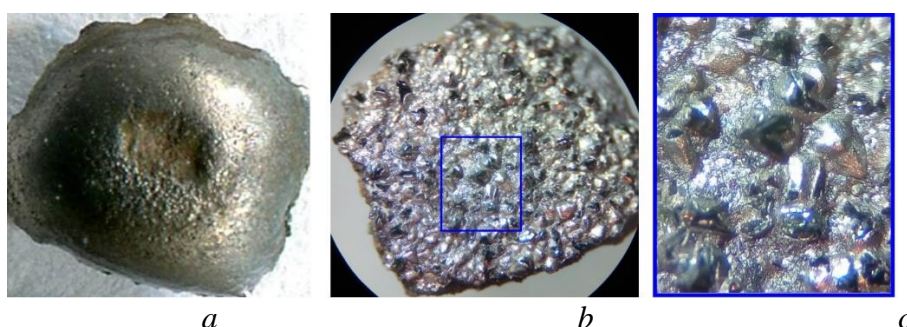


Fig. 6. Contact melting of an ARMCO-iron plate located on a graphite substrate at a pressure of 8,3 GPa: a – the shape of a drop wetting the substrate (top view); b, c – spontaneous diamond formation at the Fe-graphite interface (c – fragment highlighted in b at higher magnification)

*Melting of  $(\text{Co/Cr})_{eut}$  alloy and  $\text{Fe}_{2-4}\text{N}$  nitride at a pressure of 8,3 GPa in the absence of contact with carbon.* Melting of the  $(\text{Co/Cr})_{eut}$  alloy and iron nitride was carried out in a melting module with an NaCl medium without using a graphite substrate or diamond crystals. At the initial stages of  $(\text{Co/Cr})_{eut}$  melting, rounded shapes appear and traces of machining on the flat surface of the initial sample disappear. The melt is pulled together by an oxide film and the shape outlines are initially preserved, but at a higher temperature the melt takes the form of a round drop (fig. 7, a, b).

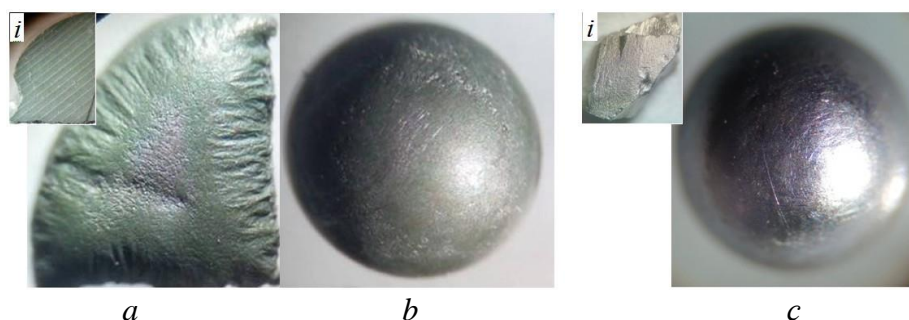


Fig. 7. Melting of the  $(\text{Co/Cr})_{eut}$  alloy (a, b) and iron nitride (c) at a pressure of 8,3 GPa in NaCl melt: a, b – successive stages of curling up of the Me melt into a drop with temperature increasing (i – an image of the initial  $(\text{Co/Cr})_{eut}$  sample with traces of machining); c – curling up of the iron nitride melt into a drop (i – an image of the initial shard from the bulk sample of remelted original powdered  $\text{Fe}_{2-4}\text{N}$  under HP-HT)

The starting iron nitride powder is identified by the supplier (Alfa Aesar GmbH) as Fe<sub>2.4</sub>N (325 mesh). According to the X-Ray powder diffraction data analysis, based on the ratio of the reflectivity of the planes for the most intense reflections, Fe<sub>2.4</sub>N consists of 53 % of Fe<sub>4</sub>N with Space Group Symmetry (SGS) *Pm3m* and approximately equal amounts of two structural varieties of Fe<sub>3</sub>N, differing in SGS – *P6<sub>3</sub>22* and *P312*. After sintering of Fe<sub>2.4</sub>N powder at high pressures ( $p \sim 8$  GPa) and temperatures ( $T_s \sim 1700$  °C) for 40 s an almost monophase polycrystalline Fe<sub>3</sub>N product with the SGS

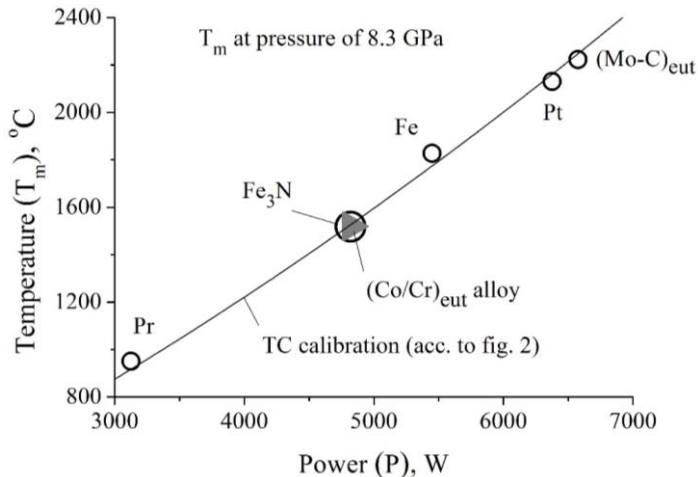


Fig. 8. Correlation of the data on the melting points of *Me* at a pressure of 8,3 GPa with the HPC thermocouple calibration (see fig. 2) and an estimate of the melting temperatures of the (Co/Cr)<sub>eut</sub> alloy and Fe<sub>3</sub>N nitride for 8,3 GPa

As can be seen the *Me* melting points referred to pressure of 8,3 GPa (see fig. 2) related with the experimentally established values of the electrical current power in the HPC heater correlate well with the of the thermocouple calibration (*TC*) curve (fig. 8).

This circumstance made it possible to estimate the melting temperatures of the (Co/Cr)<sub>eut</sub> alloy and Fe<sub>3</sub>N nitride in molten NaCl at a pressure of 8,3 GPa, which amounted to 1520 and 1518 °C, respectively. The features of the thermobaric behavior of (Co/Cr)<sub>eut</sub> and Fe<sub>3</sub>N have not been previously studied in detail. The data of [12] are the closest, the authors of which came to the conclusion that at  $p = 7$  GPa Fe<sub>3</sub>N at 1550 °C is in a molten state, but the equilibrium point associated with the onset of nitride melting has not been established.

*Experiments at reduced pressure.* The possibility of performing high-temperature experiments in HPAT-30 at pressures of less than 6 GPa created by reducing the axial compression force of the apparatus is rather limited due to an increase in the probability of explosive depressurization of the HPC, since the friction forces in the materials of the deformable seal zone inevitably become weaker. An effective way to reduce the pressure in the cell while maintaining the optimal compression force of the seals is to reduce the initial density of the pressed parts mainly from the central zone of the cell where the sample is located (see fig. 1). Of course, after this it is necessary to correct the HPC calibration including using the method of *post factum* fixation of the *Me* melting.

A decreasing of pressed parts density (see fig. 1, *a*) as: 1 (thermal insulation), 2 (axial heater), 3 (lids) and 4 (capsule) respectively by 10; 10; 15 and 15% with respect to the nominal density of the parts used in previous experiments ( $p \cong 8.3$  GPa) the pressure in the cell turns out to be significantly lower. Based on the results of experiments with melting of Pr, Al, Cu, Fe, as well as the peculiarities of diamond nucleation and grows on *Me*-graphite interface, the pressure level in the HPCI, at least in the temperature range around the melting of (Co/Cr)<sub>eut</sub> alloy, Fe<sub>3</sub>N nitride, and Fe, was estimated to be  $p \cong 6,7$  GPa.

*P6<sub>3</sub>22* structure is formed (analysis by powder diffraction after grinding the sintered sample). Note that the study of diffraction from a polycrystal revealed the strongest crystallographic texture of the material with the preferred orientation of crystallites by the (111) planes normal to the HPC compression axis. In the obtained diffraction spectrum there are no reflections except 111 and 222 of Fe<sub>3</sub>N. The density of polycrystalline Fe<sub>3</sub>N, established by the hydrostatic weighing method, is  $7,30 \pm 0,05$  g/cm<sup>3</sup>. Thus, we can assume with a high degree of certainty that the sample of this particular polymorphic modification of the compound was subjected to melting in our experiments (see fig. 7, *c*).

As an example, a comparison of two situations with the behavior of a Fe (*Armco*)–C (gr) contact pair is representative. At a pressure of  $p \cong 8,3$  GPa and a temperature of 1850 °C the system is deep in the region of diamond thermodynamic stability with the supercooling of  $\Delta T \cong 650$  °C (see fig. 3). In molten Fe the diffusion mobility of carbon is significant and, iron being an effective diamond-producing solvent-catalyst, under the indicated conditions of thermobaric action facilitates spontaneous nucleation and growth of diamond crystals (see fig. 6). At a pressure of  $p \cong 6,7$  GPa in the experiment at a temperature of 1910 °C, corresponding to the diamond-graphite equilibrium ( $\Delta T \cong 0$  °C), Fe melting was observed with the formation of a drop which wets the graphite substrate (fig. 9).

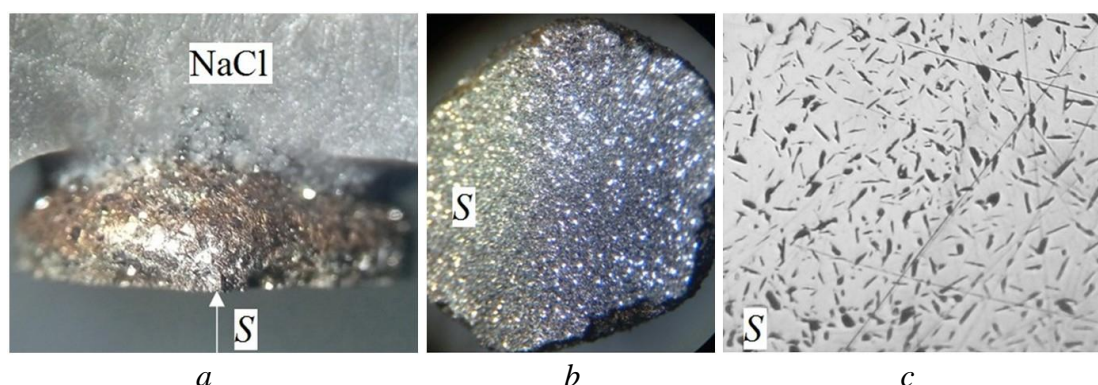


Fig. 9. Melting of *Armco*-iron in contact with the graphite substrate at a pressure of  $p \cong 6.7$  Gpa and a temperature of 1910 °C: *a* – the shape of a droplet wetting the substrate (side view); *b* – full face of the contact surface of a drop (*S*) with graphite, *c* – brightfield image of the polished section surface in an optical microscope revealing the characteristic features of the microstructure of a crystallized melt with graphite precipitates

The wetting contact angle is about 90 ° or slightly exceeds it, which corresponds to the carbon concentration ( $\alpha$ ) in the melt with  $\alpha \geq 4,3$  wt. % (eutectic value at normal pressure [13]). Evaluation of the carbon content from the increase in the mass of the sample gives a value of  $\alpha \cong 5,7$  wt. %, which may be associated with the effect of pressure on the solubility of carbon in the iron melt. Crystallization of diamonds was not observed, which indicates the transition of the system to the graphite thermodynamic stability region. A lot of specular highlights on the contact surface of the crystallized Fe–C alloy is probably due to carbide precipitates (fig. 9, *b*). The absence of diamonds, in particular, is evidenced by the low abrasion resistance of the sample surface. On a polished section in the bright field mode of an optical microscope, a microstructure is easily detected, which resembles the structure of gray cast iron with precipitates of lamellar graphite with flakes up to 100  $\mu\text{m}$  and a thickness of 20–30  $\mu\text{m}$  (see fig. 9, *c*). Of course, additional EDX studies are needed to make final conclusions about the alloy composition.

*The study of the behavior of GaN–Fe, GaN–Fe<sub>2.4</sub>N and GaN–(Co/Cr)<sub>eut</sub> contact pairs.* The technique of carrying out thermobaric research assumed the use of samples in the form of round plates with a diameter of 8 mm and a thickness of 2–3 mm, made of *Armco* iron (up to 99.9 % Fe) and (Co/Cr)<sub>eut</sub> alloy (46,5 at. % Cr). Iron nitride powder Fe<sub>2.4</sub>N ( $\leq 44$   $\mu\text{m}$ , as delivered) was preliminarily compacted in a steel mold before being placed in a capsule (see fig. 1). Compaction of difficult-to-compress polydisperse powders from hard brittle particles of gallium nitride ( $\leq 40$   $\mu\text{m}$ ) was carried out using vibration during the assembly of the capsule. Typically, the arrangement of the components involved a three-layer GaN–sample–GaN sequence, as shown in fig. 1, *a*, and less often a simplified two-layer combination with GaN over the sample.

The compression force of HPAT-30, as in the case of experiments with *Me* melting, was maintained at the nominal value  $F = 16,35$  MN. The power of the electric current in the heater was increased uniformly to the required level for 20 s. The duration of thermobaric action for all contact

pairs was 3 min. At the end of the exposure, the heating power was smoothly reduced to zero within 10 s. After a short cooling of the apparatus pressure was released during 30 s. Recovered contact pair was purified from salt residues by ultrasonic cavitation treatment in water and then in isopropyl alcohol for 3 min at each of the operations.

The mass of the sample before and after the experiment was determined with a relative error of  $\delta \approx 0,15\%$  using an AXIS AD 200 scales. A diagnostic sign of the beginning interaction between contact pair components was the increment of sample mass ( $\Delta M$ ) caused by the dissolution of GaN in the melt appeared at interphase boundary during of HP–HT action. A measuring of  $\Delta m$  is certainly possible only in the case of delaminating residual (undissolved) GaN from the *Me* sample. At this incident GaN is seceded as a sintered polycrystalline plate. The delaminating is often observed to occur spontaneously due to critical level of thermo- and baroelastic stresses between the sample and GaN plates and takes place after cooling and decompression of the HPC. Obviously, the nature of the stresses is associated with the differences in the coefficients of thermal expansion and bulk modules of the contact pair components.

A possibility of delamination, however, is often insignificant, which is associated with the influence of a number of other factors, such as the initial level of thermobaric action, changes in the physical-mechanical characteristics of the sample as a result of dissolution of GaN in it, etc. In this case, the degree of dissolution of GaN and the spatial distribution of dissolved elements can be judged by EDX, XRD and other methods.

*The GaN–Fe contact pair.* After performing of the thermobaric loadings at  $p = 8,3$  GPa in the temperature range of 1400–2000 °C the delaminating of the undissolved part of GaN occurred regardless of the type of contact pair assembly (two- or three-layered). In experiments with a pressure of 6,7 GPa delaminating was observed only in two-layer assemblies, except for the case with a maximum temperature of  $p, T$ -treatment at 2100 °C at which the melt began to coalesce into a drop (fig. 10).

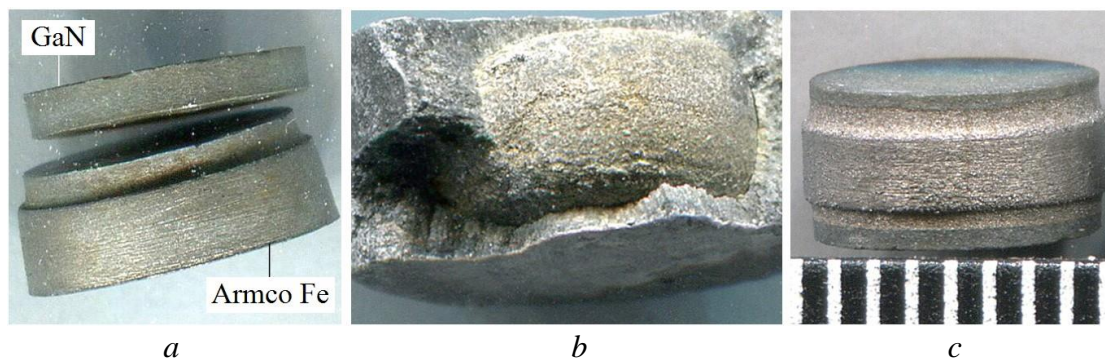


Fig. 10. An external shape of GaN–Fe contact pairs produced under pressure of 6.7 GPa at different temperatures during 3 minutes: a, b – 1680 °C and 2100 °C, respectively (two-layer GaN–sample assembly); c – 1700 °C (three-layer GaN–sample–GaN assembly); scale division is 1 mm

At similar conditions of HP–HT treatment with a three-layer assembly in all 7 fulfilled experiments at temperatures of 1700; 1840; 1910; 1965; 2020; 2080 and 2140 °C sintered bodies were recovered without any signs of delamination of contacting components (see fig. 10, c).

*The GaN–Fe<sub>2-4</sub>N contact pair.* The initial Fe<sub>2-4</sub>N and GaN powders were placed in the capsule in a compacted state one above the other so that the phase boundary remained as flat as possible. As shown above, at pressure of 8.3 GPa the melting temperature of pure Fe<sub>3</sub>N (remelted Fe<sub>2-4</sub>N) is  $T_m \cong 1518$  °C. Contact pairs were processed by temperatures of 1145; 1290; 1435; 1600 and 1765 °C. The effect of delamination of GaN from the sample was observed only in the first two experiments.

In the last sintered bodies turned out. On the lateral surface of the cylindrical samples a location of initial interface between the  $\text{Fe}_{2-4}\text{N}$  and GaN is clearly visible.

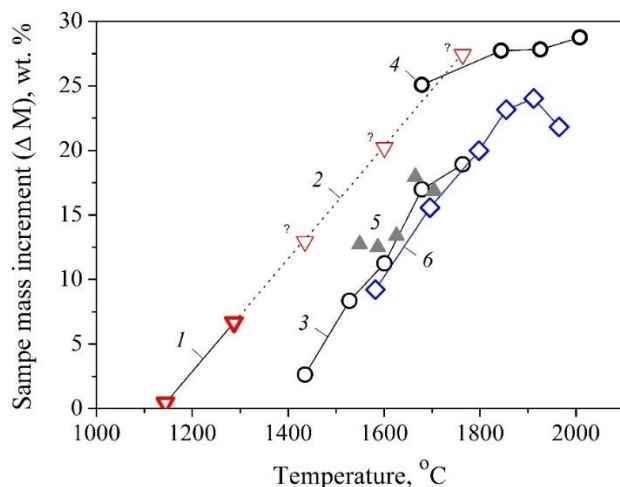


Рис. 11. The mass increment of the samples in the contact pairs as a result of their interaction with GaN under the HP-HT action at duration of 180 s: 1 – GaN– $\text{Fe}_{2-4}\text{N}$ ,  $p = 8,3$  GPa; 2 – GaN– $\text{Fe}_{2-4}\text{N}$ ,  $p = 8,3$  GPa (expected relationship for samples with non separated GaN plates); 3 – GaN–Fe,  $p = 8,3$  GPa; 4 – GaN–Fe–GaN,  $p = 8,3$  GPa; 5 – GaN– $(\text{Co/Cr})_{eut}$ –GaN,  $p = 8,3$  GPa; 6 – GaN– $(\text{Co/Cr})_{eut}$ –GaN,  $p = 6,7$  GPa

contact pairs were obtained proceeding from the  $\Delta M$  values in those cases when delamination of excess undissolved GaN took place (fig. 11).

*Final comments.* The data obtained indicate not only the fact of GaN dissolution in iron,  $\text{Fe}_3\text{N}$  nitride (sample is a remelted  $\text{Fe}_{2-4}\text{N}$  powder) and  $(\text{Co/Cr})_{eut}$  alloy but also a significant influence of the  $p$ ,  $T$ ,  $t$ -parameters of HP-HT action on a degree of dissolution. At the pressures of 6,7 and 8,3 GPa melting point of Fe is 1782 and 1827 °C, respectively. According to our estimates, at a pressure of 8,3 GPa, melting of  $\text{Fe}_3\text{N}$  and  $(\text{Co/Cr})_{eut}$  alloy occurs at much lower temperatures of 1518 and 1520 °C, respectively. The dissolution of GaN in the samples is observed even at lower temperatures, which is probably associated with the effects of contact (eutectic) melting at the interface with the sample in the studied pairs (see fig. 11). On the example of a  $(\text{Co/Cr})_{eut}$  alloy, one can observe a tendency towards a decrease in the solubility of GaN with decreasing pressure. For example, for the temperature of 1600 °C with a pressure decrease from 8,3 to 6,7 GPa (by 19,3 %) the change in the sample mass due to GaN dissolution also becomes less by about 20 %. The influence of temperature on the degree of dissolution of GaN is much more effective. Thus, at fixed pressure of  $p = 6,7$  GPa a temperature increasing from 1600 to 1900 °C (by 18,8 %) leads to GaN dissolution growth up to 160 %.

Regarding the equilibrium concentrations of Ga and N in melts of Fe,  $\text{Fe}_{2-4}\text{N}$  and  $(\text{Co/Cr})_{eut}$  alloy the final conclusion will be received after examination of quenched samples by EDX, XRD, Raman spectroscopy and other methods. A study of the features of the GaN dissolution profiles and the nature of inhomogeneities in the structure of the samples can indicate the development of processes of spontaneous nucleation and growth of GaN, as well as co-crystallization of accompanying phases, upon cooling of nonequilibrium supersaturated states of solutions in the systems under study.

**Acknowledgments.** Authors are sincere grateful Prof. S. Porowski and Prof. I. Grzegory from Institute of High Pressure Physics, Polish Academy of Sciences; academician V. Z. Turkevich from

*The GaN– $(\text{Co/Cr})_{eut}$  contact pair.* In all experiments a three-layered GaN– $(\text{Co/Cr})_{eut}$ –GaN assembly was applied (fig. 1, a). The HP-HT actions were carried out at pressures of 8,3 and 6,7 GPa. In the first case temperatures of 1550; 1590; 1630; 1665; 1700 °C, and in the second 1580; 1700; 1800; 1855; 1910 and 1965 °C were used. According to our preliminary data, the melting point of the  $(\text{Co/Cr})_{eut}$  alloy at a pressure of 8,3 GPa is  $T_m \cong 1520$  °C. In both series of experiments the sintered polycrystalline plates of undissolved GaN were easily separated from the central samples of a three-layer assembly.

The final results on the degree of GaN dissolution in the samples for each of the GaN–Fe, GaN– $\text{Fe}_{2-4}\text{N}$  and GaN– $(\text{Co/Cr})_{eut}$

V. M. Bakul Institute for superhard materials of the National Academy of Sciences of Ukraine for the valuable scientific discussion on the formulation of the problem and interpretations of obtained results; N. M. Belyavina from Taras Shevchenko National University of Kyiv for performed X-ray analysis. This study has been supported by the Grant OPUS 12 No 2016/23/B/ST5/02728 of the Polish National Science Center and additionally a number of investigations were performed as part of the project-winner of the competition «Support to research of leading and young scientists» for research and development «Gallium nitride single crystals: high pressure, structure, properties», funded by the National Research Foundation of Ukraine (project registration number - 2020.02/0078) what are greatly acknowledged.

І. А. Петруша<sup>1</sup>, Б. С. Садовий<sup>2,3</sup>, П. С. Садовий<sup>2</sup>, О. С. Осіпов, Ю. Ю. Румянцева<sup>1</sup>,  
П. А. Балабанов<sup>4</sup>, П. Клімчик<sup>5</sup>, Ю. І. Садова, О. В. Савицький, С. О. Гордєєв, Т. О. Сакал<sup>1</sup>

<sup>1</sup>Інститут надтвердих матеріалів імені В. М. Бакуля НАН України

<sup>2</sup>Інститут фізики високих тисків ПАН, Польща

<sup>3</sup>Львівський національний університет імені Івана Франка, Україна

<sup>4</sup>ТОВ ЕкоДаймонд, Німеччина

<sup>5</sup>Інститут передових технологій обробки, Польща

#### ВИВЧЕННЯ ПОВЕДІНКИ GaN У КОНТАКТІ З Fe, Fe<sub>2-4</sub>N і Co/Cr ПРИ ВИСОКИХ ТИСКАХ І ТЕМПЕРАТУРАХ

В роботі описані особливості поведінки нітриду галію (GaN), що знаходиться у контакті з Fe, Fe<sub>2-4</sub>N і (Co/Cr)<sub>евт</sub> в умовах високих тисків ( $p \cong 6-8$  ГПа) і температур до 2000 °С. Детально висвітлені підготовчі етапи експериментального дослідження, що включають термобаричне градування апарату високого тиску тороїдального типу за допомогою термопари з урахуванням результатів з плавлення ряду металів, сплавів та їх сполук, таких як Pt, (Mo-C)<sub>евт</sub>, Fe, Fe<sub>2-4</sub>N, (Co/Cr)<sub>евт</sub>, Cu, і Pr. Встановлено, що GaN розчиняється розплавах Fe, Fe<sub>2-4</sub>N і (Co/Cr)<sub>евт</sub>, при цьому спостерігається закономірне збільшення маси зразків. Як правило, зміна маси фіксується при температурах нижче температури плавлення чистого матеріалу (зразка), що вказує на виникнення процесів міжфазного контактного плавлення на границі поділу GaN-зразок. При фіксованому тиску і ізохронних умов експерименту ступінь розчинення GaN сильно залежить від температури для всіх розглянутих систем. В області температур 1800–2000 °С зміна маси другого компонента в контактних парах GaN–Fe, GaN–Fe<sub>2-4</sub>N і GaN–(Co/Cr)<sub>евт</sub> в наслідок розчинення GaN досягає 20–30 мас. %. На прикладі сплаву (Co/Cr)<sub>евт</sub> демонструється тенденція до зменшення розчинності GaN з пониженням тиску. Висновки щодо досягнення рівноважних концентрацій Ga і N в розплавах Fe, нітриду Fe<sub>2-4</sub>N і сплаву (Co/Cr)<sub>евт</sub> будуть отримані після досліджень загартованих зразків із застосуванням методів EDX, XRD, спектроскопії комбінаційного розсіювання та ін.

**Ключові слова:** нітрид галію, високий тиск і висока температура, контактне плавлення, розчинення в розплавах, залізо, нітрид заліза, сплав Co/Cr

І. А. Петруша<sup>1</sup>, Б. С. Садовий<sup>2,3</sup>, П. С. Садовий<sup>2</sup>, А. С. Осіпов, Ю. Ю. Румянцева<sup>1</sup>,  
П. А. Балабанов<sup>4</sup>, П. Клімчик<sup>5</sup>, Ю. І. Садовая, А. В. Савицький, С. А. Гордєєв, Т. А. Сакал<sup>1</sup>

<sup>1</sup>Інститут сверхтвердых материалов имени В. Н. Бакуля НАН Украины

<sup>2</sup>Інститут фізики високих давлень ПАН, Польща

<sup>3</sup>Львовский национальный университет имени Ивана Франко, Украина

<sup>4</sup>ООО ЭкоДаймонд, Германия

<sup>5</sup>Інститут передових технологій обробки, Польща

#### ИССЛЕДОВАНИЕ ПОВЕДЕНИЯ GaN В КОНТАКТЕ С Fe, Fe<sub>2-4</sub>N И Co/Cr ПРИ ВЫСОКИХ ДАВЛЕНИЯХ И ТЕМПЕРАТУРАХ

В работе описаны особенности поведения нитрида галлия (GaN), находящегося в контакте с Fe, Fe<sub>2-4</sub>N и (Co/Cr)<sub>евт</sub> в условиях высоких давлений ( $p \cong 6-8$  ГПа) и температур до 2000 °С. Подробно

освещены подготовительные этапы экспериментального исследования, включающие термобарическое градуирование аппарата высокого давления тороидального типа с помощью терморпары с учетом результатов по плавлению ряда металлов, сплавов и их соединений, таких как Pt, (Mo-C)<sub>эвт.</sub>, Fe, Fe<sub>2-4</sub>N, (Co/Cr)<sub>эвт.</sub>, Cu, и Pr. Установлено, что GaN растворяется в расплавах Fe, Fe<sub>2-4</sub>N и (Co/Cr)<sub>эвт.</sub>, при этом наблюдается закономерное увеличение массы образцов. Как правило, изменение массы фиксируется при температурах ниже температуры плавления чистого материала (образца), что указывает на возникновение процессов межфазного контактного плавления на границе раздела GaN-образец. При фиксированном давлении и изохронных условиях эксперимента степень растворения GaN сильно зависит от температуры для всех рассматриваемых систем. В области температур 1800–2000 °С изменение массы второго компонента в контактных парах GaN-Fe, GaN-Fe<sub>2-4</sub>N и GaN-(Co/Cr)<sub>эвт.</sub> вследствие растворения GaN достигает 20–30 масс. %. На примере сплава (Co/Cr)<sub>эвт.</sub> демонстрируется тенденция к уменьшению растворимости GaN с понижением давления. Выводы относительно достижения равновесных концентраций Ga и N в расплавах Fe, нитрида Fe<sub>2-4</sub>N и сплава (Co/Cr)<sub>эвт.</sub> будут получены после исследований закаленных образцов с применением методов EDX, XRD, спектроскопии комбинационного рассеяния и др.

**Ключевые слова:** нитрид галлия, высокое давление и высокая температура, контактное плавление, растворение в расплавах, железо, нитрид железа, сплав Co/Cr

### Література

1. Khvostantsev L. G., Slesarev V. N., Brazhkin V. V. Toroid type high-pressure device: history and prospects // High Pressure Res. – 2004. – V. 24, N 3. – P. 371–383; doi:10.1080/08957950412331298761.
2. Балабанов П. А., Klimczyk P., Cygan S. Применение импульсного тока высокой частоты для нагрева аппарата высокого давления «тороид-30» // Породоразрушающий и металлообрабатывающий инструмент – техника, технология его изготовления и применения. Сб. науч. тр. – Вып. 19. – К.: ИСМ им. В.Н. Бакуля НАН Украины, 2016. – С. 181–184.
3. Errandonea D. High-pressure melting curves of the transition metals Cu, Ni, Pd, and Pt // Phys. Rev. B. – 2013. – V. 87. – P. 054108 (1–5); doi.org/10.1103/PhysRevB.87.054108.
4. Кублий В. З., Великанова Т. Я. Новые данные о диаграмме состояния Мо-С // Диаграммы состояния карбид- и нитридсодержащих систем: книга; НАН Украины. Ин-т проблем материаловедения. – Киев, 1981: –С. 79–88.
5. Контактне плавлення молибдену в умовах високого тиску / І. А. Петруша, М. В. Нікішина, О. І. Кириченко и др. // Синтез, спекание и свойства сверхтвердых материалов. Сб. науч. тр. / Ин-т сверхтвердых материалов им. В.Н. Бакуля НАН Украины; – К.: Логос, 2010. – С. 136–146.
6. Fateeva N. S., Vereshchagin L. F. Melting curve of molybdenum at 90 kbar // JETP Lett. English Transl. – 1974. – V. 14. – P. 153–155.
7. Berman R. The diamond-graphite equilibrium calculation: the influence of a recent determination of the Gibbs energy difference // Solid State Commun. –1996. – V. 99, N 1. – P. 35–37; doi.org/10.1016/0038-1098(96)00171-8.
8. The challenge of decomposition and melting of gallium nitride under high pressure and high temperature / S. Porowski, B Sadovyi, S. Gierlotka et al. // J. Phys. Chem. Solids. – 2015. – V. 85. – P. 138–143; doi.org/10.1016/j.jpcs.2015.05.006.
9. Фазовые превращения соединений при высоком давлении: справ. изд.: в 2-х кн. / Е. Ю. Тонков; под ред. Е. Г. Понятовского. – М.: Металлургия, 1988. – Кн. 1: 358 с.; Кн. 2: 464 с.
10. Диаграммы плавкости солевых систем: справ. изд.: в 2-х частях; Ч. 1: Двойные системы с общим анионом / В. И. Посыпайко, Е. А. Алексеева, Н. А. Васина и др. – М.: Металлургия, 1977. – 416 с.

11. Measurement of Rh-C, Pt-C and Ru-C eutectic points by four national metrology institutes / Y. Yamada, Y. Duan, M. Ballico et al. // *Metrologia*. – 2001. – V. 38, N 3. – P. 203–211; doi:10.1088/0026-1394/38/3/2.
12. HPHT synthesis of diamond with high nitrogen content from an Fe<sub>3</sub>N–C System / Yu. Borzdov, Yu. Pal'yanov, I. Kupriyanov et al. // *Diamond Relat. Mater.* – 2002. – V. 11. – P. 1863–1870; doi:10.1016/s0925-9635(02)00184-x.
13. Исследование процесса взаимодействия стали с графитом при контактно-реактивной пайке / Т. А. Кокина, Г. А. Каравецкий, Л. В. Леонов и др. // *Конструкционные материалы на основе углерода*. – 1975. – № 10. – С. 176–182.

Received 16.08.2021

## References

1. Khvostantsev, L. G., Slesarev, V. N., & Brazhkin, V. V. (2004). Toroid type high-pressure device: history and prospects. *High Pressure Research*, 24, 3, 371–383.
2. Balabanov, P. A., Klimczyk, P., & Cygan, S. (2016). Primenenie impulsnogo toka vysokoi chastoty dlia apparata vysokogo davleniia [Application of pulse current high frequency for heating of apparatus of high pressure «toroid-30»]. *Porodorazrushaiushchii i metalloobrabatyvaiushchii instrument – tekhnika i tekhnologiia ego izgotovleniia i primeneniia – Rock Destruction and Metal-Working Tools – Techniques and Technology of the Tool Production and Applications*, 19, 181–184 [in Russian].
3. Errandonea, D. (2013). High-pressure melting curves of the transition metals Cu, Ni, Pd, and Pt. *Phys. Rev. B.*, 87, 054108 (1–5).
4. Kublii, V. Z., & Velikanova, T. Ya. (1981). Novye dannye o diagramme sostoianii Mo–C [New data on the state diagram of Mo–C]. *Diagrammy sostoianii karbid- i nitridsoderzhashchikh sistem [State diagrams of carbide- and nitride-containing systems]* Kyiv, NAS of Ukraine, IPMS [in Russian].
5. Petrusha, I. A., Nikishina, M. V., Kirichenko O. I., et al. (2010). Kontaktne plavlennia molibdenu v umovakh vysokogo tysku [Contact melting of the molybdenum under high pressure]. *Sintez, spekanie i svoistva sverhtverdyh materialov – Synthesis, sintering and properties of superhard materials*. Kyiv, NAS of Ukraine, ISM, Logos [in Ukrainian].
6. Fateeva, N. S., & Vereshchagin L. F (1974). Melting curve of molybdenum at 90 kbar. *JETP Lett. English Transl.*, 14, 153.
7. Berman, R. (1996). The diamond-graphite equilibrium calculation: the influence of a recent determination of the Gibbs energy difference. *Solid State Comm.*, 99, 1, 35–37.
8. Porowski, S., Sadovyi, B., Gierlotka, S., et al. (2015). The challenge of decomposition and melting of gallium nitride under high pressure and high temperature. *J. Phys. Chem. Solids*, 85, 138–143.
9. Tonkov, E. Yu. (1988). *Fazovye prevrashcheniia soedinenii pri vysokom davlenii [Phase transformations of compounds at high pressure]*. (Vols. 1, 2). Moscow: Metallurgiiia [in Russian].
10. Posypaiko, V. I., Alekseeva, E. A. Vasina, N. A., et al. (1977). *Diagrammy plavkosti solevikh sistem: Dvoinye sistemy s obshchim anionom. (Parts 1, 2). [Diagrams of the melting of salt systems: Binary systems with a common anion]*. (Part 1). Moscow: Metallurgiiia [in Russian].
11. Yamada, Y., Duan, Y., Ballico, M., et al. (2001). Measurement of Rh–C, Pt–C and Ru–C eutectic points by four national metrology institutes. *Metrologia*, 38, 3, 203–211.
12. Borzdov, Yu., Pal'yanov, Yu., Kupriyanov, I., et al. (2002). HPHT synthesis of diamond with high nitrogen content from an Fe<sub>3</sub>N–C System. *Diamond Relat. Mater.*, 11, 1863–1870.

13. Kokina, T. A., Karavetskii, G. A., Leonov, L. V., et al. (1975). Issledovanie protsessa vzaimodeistviia stali s grafitom pri kontaktno-reaktivnoi paike [Investigation of the interaction process of steel with graphite at contact-reactive brazing]. *Konstruktivnye materialy na osnove uhleroda – Carbon-based structural materials*, 10, 176–182 [in Russian].

УДК 661.868.1:004.94:62-987

DOI: 10.33839/2708-731X-24-1-325-334

**О.П. Людвіченко**, асп.; **О.М. Анісін**, м.н.с.;  
**О.О. Лещук, І. А. Петруша**, доктора технічних наук

*Інститут надтвердих матеріалів ім. В.М. Бакуля НАН України, вул. Автозаводська, 2  
04074, м. Київ e-mail: ludvial@ukr.net*

### **МОДЕЛЮВАННЯ ТЕПЛОВОГО СТАНУ АПАРАТА ВИСОКОГО ТИСКУ ПРИ ДОСЛІДЖЕННІ РОЗЧИННОСТІ НІТРИДУ ГАЛІЮ В ЗАЛІЗІ**

*З використанням комп'ютерного моделювання досліджено тепловий стан комірки апарата високого тиску, що використовують для визначення розчинності нітриду галію у залізі. Результати розрахунків представлені стаціонарними температурними полями в різних елементах апарата. Отримано, що при температурі в контрольній точці комірки в 1800 °С максимальний її перепад в об'ємі досліджуваних зразків нітриду галію і заліза становить 25 °С. Змодельована конфігурація комірки і визначені для неї умови нагрівання є прийнятними для експериментальних досліджень розчинності GaN в контакті із Fe в умовах високих тисків і температур.*

**Ключові слова:** нітрид галію, апарат високого тиску, комірка високого тиску, метод скінченних елементів.

Нітрид галію – це широкосмуговий напівпровідник, що в теперішній час має зростаюче технологічне застосування. Так, в 2014 р. за винахід ефективних блакитних світлодіодів на основі GaN, що привели до появи яскравих та енергозберігаючих білих джерел світла, присуджено Нобелівську премію з фізики. Виготовлення таких світлодіодів потребує наявності монокристалічних підкладок з GaN для їх епітаксialного нарощування.

Створення ефективного способу кристалізації GaN є актуальним питанням, оскільки його фізичні властивості значною мірою визначаються виникненням різних дефектів. Серед методів вирощування GaN відома гідридна парофазна епітаксія, що дозволяє кристалізувати GaN при атмосферному тиску та температурі 1000 °С зі швидкістю біля 100 мкм/год. Недосконалістю цього методу є висока дефектність вирощених кристалів, що виникає внаслідок залишкового напружено-деформованого стану як в кристалах, так і в підкладках, на яких вони зростають.

Іншим методом вирощування кристалів GaN є амонотермія з використанням надкритичного аміаку (NH<sub>3</sub>) як розчинника для GaN при тиску 0,2–0,3 ГПа та температурі 600–800 °С. Серйозним недоліком цього методу є надзвичайно низька швидкість росту (1–2 мкм/год) та відносно низька чистота вирощених кристалів.

Перші високоякісні кристали GaN, які можуть бути використані для епітаксialного нарощування та виготовлення процесорних пристроїв, були отримані при температурі 1500 °С і тиску азоту 1 ГПа в газостатичній установці в Інституті фізики високих тисків Польської академії наук.

Новим підходом в отриманні нітриду галію є його кристалізація із багатокомпонентної розчин-розплавної системи Fe–Ga–N при високих тисках (~ 6 ГПа) і температурах (~ 1800 °С). Основною проблемою при розробці комірки до апарату високого тиску (АВТ) є